 CMES, vol.32, no.3, pp.161-174, 2008

Analysis of Transient Heat Conduction in 3D Anisotropic Functionally Graded Solids, by the MLPG Method

J. Sladek[1], V. Sladek[1], C.L. Tan[2] and S.N. Atluri[3]

Abstract: A meshless method based on the local Petrov-Galerkin approach is proposed for the solution of steady-state and transient heat conduction problems in a continuously non-homogeneous anisotropic medium. The Laplace transform is used to treat the time dependence of the variables for transient problems. The analyzed domain is covered by small subdomains with a simple geometry. A weak formulation for the set of governing equations is transformed into local integral equations on local subdomains by using a unit test function. Nodal points are randomly distributed in the 3D analyzed domain and each node is surrounded by a spherical subdomain to which a local integral equation is applied. The meshless approximation based on the Moving Least-Squares (MLS) method is employed for the implementation. Several example problems with Dirichlet, mixed, and/or convection boundary conditions, are presented to demonstrate the veracity and effectiveness of the numerical approach.

Keyword: meshless method, local weak form, Heaviside step function, moving least squares interpolation, Laplace transform

1 Introduction

Functionally graded materials are multi-phase materials with the phase volume fractions varying gradually in space, in a pre-determined profile. This results in continuously graded thermo-mechanical properties at the (macroscopic) structural scale. Often, these spatial gradients in material behaviour render FGMs as superior to conventional composites. FGMs possess some advantages over conventional composites because of their continuously graded structures and properties [Suresh and Mortensen (1998); Miyamoto et al. (1999)]. FGMs may exhibit isotropic or anisotropic material properties, depending on the processing technique and the practical engineering requirements. Recent progress in the development and research of FGMs has also enhanced interests in the development of numerical methods for the solution of heat conduction problems in continuously non-homogeneous solids. The literature on heat conduction problems in FGM materials has focused mainly on problems with exponential variations of thermal properties, formulated in Cartesian coordinates and under steady-state boundary conditions [Noda and Jin (1993); Erdogan and Wu (1996); Jin and Noda (1993)]. Transient heat transfer in FGMs with the exponential spatial variation has also been examined, but to a lesser extent [Jin and Batra, 1996; Noda and Jin (1994); Jin and Paulino (2001); Sutradhar et al. (2002); Jin (2002)].

Due to the high mathematical complexity of the initial-boundary value problems, analytical approaches for the thermo-mechanics of FGMs are restricted to simple geometries and boundary conditions. Transient heat conduction analysis in FGM demands accurate and efficient numerical methods. The finite element method (FEM) can be successfully applied to problems with an arbitrary variation of material properties by using special graded elements [Kim and Paulino (2002)]. In commercial computer codes, however, material properties are considered to be uniform on each element. The boundary element method (BEM) is also a suitable numerical tool for this

[1] Institute of Construction and Architecture, Slovak Academy of Sciences, 84503 Bratislava, Slovakia
[2] Department of Mechanical & Aerospace Engineering, Carleton University, Ottawa, Canada K1S 5B6
[3] Center of Aerospace Research & Education, University of California at Irvine, Irvine, CA 92697-3975, USA

purpose. The heat conduction problem in a homogeneous body with isotropic material properties has been successfully solved by the BEM very frequently in the literature [Brebbia et al. (1984)]. A pure boundary formulation is also available for anisotropic media [Chang et al. (1973)]. However, the fundamental solution for continuously non-homogeneous bodies is not available in general. If an exponential spatial variation of material properties is considered, one can derive the fundamental solution for heat conduction problems [Sutradhar et al. (2002)]. One possibility to obtain a BEM formulation is based on the use of fundamental solutions for a fictitious homogeneous medium, as has been suggested for the first time by Butterfield (1978) for potential flow problems. This approach, which is the basis of the global BEM, however, leads to a boundary-domain integral formulation with additional domain integrals for the gradients of primary fields to obtain a unique formulation. Such an integral formulation has been applied to the heat conduction analysis in non-homogeneous media by Tanaka and Tanaka (1980). The price to be paid in such an approach is the loss of a pure boundary integral character of the formulation; in addition, evaluation of the integrals on the global domain presents some computational difficulties. Notwithstanding the great success of the finite and boundary element methods as effective numerical tools for the solution of boundary and initial value problems in engineering applications, there remains shortcomings of these methods. This has generated growing interest in developing new advanced computational methods.

Meshless formulations, in particular, are becoming popular due to their high adaptivity and a low cost to prepare input data for numerical analyses. A significant number of such methods have been proposed so far [Belytschko et al. (1996); Atluri and Zhu(1998), Atluri and Shen (2002); Atluri (2004)]. In conventional discretization methods, there is a discontinuity of secondary fields (gradients of primary fields) at the interface of elements. For modeling continuously non-homogeneous solids, the approach based on piecewise continuous elements will introduce some inaccuracies. Therefore, modeling based on C^1 continuity, such as using meshless methods, is expected to be more accurate than conventional discretization techniques. The meshless local Petrov-Galerkin (MLPG) method is a fundamental base for the derivation of many meshless formulations, since the trial and the test functions can be chosen from different functional spaces. Recent successes of the MLPG methods have been reported in the development of the MLPG finite-volume mixed method [Atluri, Han, and Rajendran (2004)], which was later extended to finite deformation analysis of static and dynamic problems [Han et al (2005)]; in simplified treatment of essential boundary conditions by a novel modified MLS procedure [Gao et al. (2006)]; in analysis of transient thermo-mechanical response of functionally gradient composites [Ching and Chen (2006)]; in the development of the mixed scheme to interpolate the elastic displacements and stresses independently [Atluri et al (2006a), (2006b)]; in proposal of a direct solution method for the quasi-unsymmetric sparse matrix arising in the MLPG [Yuan et al. (2007)]; and, in the development of the MLPG using the Dirac delta function as the test function for 2D heat conduction problems in irregular domain [Wu et al. (2007)]. The local integral formulations with the use of a suitable fundamental solution have been successfully applied to potential problems [Zhu et al. (1998); Mikhailov (2002)], isotropic elastostatics [Atluri et al. (2000); Sladek et al. (2000)], elastodynamics [Sladek et al. (2003a,b)], heat conduction [Sladek et al. (2003c,d)], thermoelasticity [Sladek et al. (2001)] and plate/shell problems [Long and Atluri (2002); Sladek et al. (2002)] in homogeneous and non-homogeneous solids. Applicability of the MLPG is enhanced if a simple unit function is used as the test function in the local weak form. The method has been successfully applied to transient heat conduction problems in 2D with anisotropic and continuously non-homogeneous solids [Sladek et al. (2004a,b)], and to elasticity [Sladek et al. (2004c); Sellountos et al. (2005)], plate and shell structures [Soric et al. (2004); Sladek et al. (2007c, 2008)] and smart materials [Sladek et al. (2007b)]. In all the above- mentioned papers,

the MLPG has been applied to 2D problems. The application of meshless methods to 3D problems has, hitherto, been very limited indeed. In this regard, Han et al. (2004a,b) have applied MLPG to elasticity and the present authors have recently analyzed 3D axisymmetric heat conduction problems using the same MLPG approach [Sladek et al. (2003d, 2007a)].

In this paper, the meshless local Petrov-Galerkin (MLPG) method is applied to transient heat conduction problems in 3D solids with continuously non-homogeneous and anisotropic material properties. The Laplace transform technique is applied to eliminate the time variable in the differential equation. The original linear parabolic differential equation is converted into a linear elliptic partial differential equation. Small spherical subdomains surrounding the nodes are randomly distributed over the analyzed domain. A unit step function is chosen as the test function to derive local integral equations on boundaries of the chosen subdomains. For transient heat conduction problem the local integral equations (LIE) have a boundary-domain integral form. Only for a steady-state problem can a pure surface integral formulation on local boundaries be obtained. However, the boundary-domain integral formulation on simple subdomains does not imply any difficulties. The local integral equations are non-singular and take a very simple form. Spatial variation of the Laplace transforms and the heat flux on the subdomain are approximated by means of the moving least-squares (MLS) method. Several quasi-static boundary value problems are solved for various values of the Laplace transform parameter. The Stehfest (1970) numerical inversion method is applied to obtain the time-dependent solutions. Numerical examples are presented to verify the proposed numerical method.

2 Local integral equations for transient heat conduction problems

Consider a boundary value problem for heat conduction in a continuously non-homogeneous anisotropic medium, which is governed by the following equation:

$$\rho(\mathbf{x})c(\mathbf{x})\frac{\partial\theta}{\partial t}(\mathbf{x},t)=\left[k_{ij}(\mathbf{x})\theta_{,j}(\mathbf{x},t)\right]_{,i}+Q(\mathbf{x},t), \tag{1}$$

where $\theta(\mathbf{x},t)$ is the temperature field, $Q(\mathbf{x},t)$ is the density of body heat sources, k_{ij} is the thermal conductivity tensor, $\rho(\mathbf{x})$ is the mass density and $c(\mathbf{x})$ the specific heat.

The global boundary Γ consists of three parts $\Gamma=\Gamma_\theta\cup\Gamma_q\cup\Gamma_3$ and the following boundary and initial conditions are assumed

$$\begin{aligned}
&\theta(\mathbf{x},t)=\tilde{\theta}(\mathbf{x},t)\text{ on }\Gamma_\theta\\
&q(\mathbf{x},t)=k_{ij}(\mathbf{x})\theta_{,j}(\mathbf{x},t)n_i\\
&(\mathbf{x})=\tilde{q}(\mathbf{x},t)\text{ on }\Gamma_q\\
&q(\mathbf{x},t)=h(\mathbf{x})\left[\theta_e(t)-\theta(\mathbf{x},t)\right]\text{ on }\Gamma_3\\
&\theta(\mathbf{x},t)|_{t=0}=\theta(\mathbf{x},0)
\end{aligned} \tag{2}$$

where n_i is the unit outward normal of the global boundary, $h(\mathbf{x})$ is the heat transfer coefficient, $\theta_e(t)$is the temperature of the fluid medium outside of solid body, Γ_θ is the part of the global boundary with prescribed temperature and on Γ_q the flux is prescribed (Fig. 1). The part Γ_3 represents the surface where convective boundary condition is prescribed.

Applying the Laplace transform

$$L\left[\theta(\mathbf{x},t)\right]=\overline{\theta}(\mathbf{x},s)=\int_0^\infty\theta(\mathbf{x},t)e^{-st}dt,$$

to the governing equation (1), we have

$$\left[k_{ij}(\mathbf{x})\overline{\theta}_{,j}(\mathbf{x},s)\right]_{,i}-\rho(\mathbf{x})c(\mathbf{x})s\overline{\theta}(\mathbf{x},s)=-\overline{F}(\mathbf{x},s), \tag{3}$$

where

$$\overline{F}(\mathbf{x},s)=\overline{Q}(\mathbf{x},s)+\theta(\mathbf{x},0)$$

is the re-defined body heat source in the Laplace transform domain with initial boundary condition for temperature and s is the Laplace transform parameter.

Instead of writing the global weak form for the above governing equation, the MLPG methods

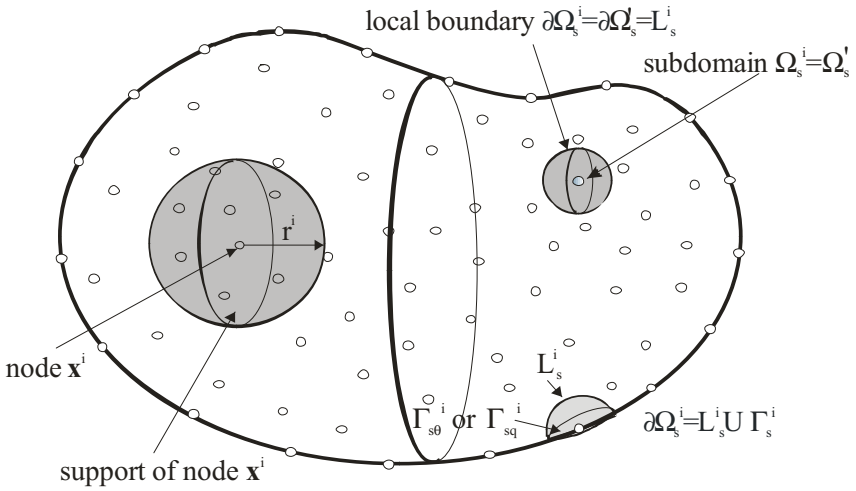

Figure 1: Local boundaries for weak formulation and support domain of weight function at node $\mathbf{x}^i$

construct the weak form over local subdomains such as Ω_s, which is a small region taken for each node inside the global domain [Sladek et al. (2004a)]. The local subdomains overlap each other, and cover the whole global domain Ω. The local subdomains could be of any geometric shape and size. In this paper, the local subdomains are taken to be of spherical shape. The local weak form of the governing equation (2) can be written as

$$\int_{\Omega_s^i}\Big[\left(k_{ij}(\mathbf{x})\overline{\theta}_{,j}(\mathbf{x},s)\right)_{,i}-\rho(\mathbf{x})c(\mathbf{x})s\overline{\theta}(\mathbf{x},s) +\overline{F}(\mathbf{x},s)\Big]\theta^*(\mathbf{x})d\Omega=0 \quad , \quad (4)$$

where $\theta^*(\mathbf{x})$ is a weight (test) function.

Applying the Gauss divergence theorem to eq. (4) one can write

$$\int_{\partial\Omega_s^i}\overline{q}(\mathbf{x},s)\theta^*(\mathbf{x})d\Gamma-\int_{\Omega_s^i}k_{ij}(\mathbf{x})\overline{\theta}_{,j}(\mathbf{x},s)\theta^*_{,i}(\mathbf{x})d\Omega -\int_{\Omega_s^i}\rho(\mathbf{x})c(\mathbf{x})s\overline{\theta}(\mathbf{x},s)\theta^*(\mathbf{x})d\Omega +\int_{\Omega_s^i}\overline{F}(\mathbf{x},s)\theta^*(\mathbf{x})d\Omega=0, \quad (5)$$

where $\partial\Omega_s$ is the boundary of the local subdomain and

$$\overline{q}(\mathbf{x},s)=k_{ij}(\mathbf{x})\overline{\theta}_{,j}(\mathbf{x},s)n_i(\mathbf{x}).$$

The local weak form, eq. (5), is a starting point to derive local boundary integral equations if an appropriate test function is selected. If a Heaviside step function is chosen as the test function $\theta^*(\mathbf{x})$ in each subdomain

$$\theta^*(\mathbf{x})=\begin{cases}1 & \text{at } \mathbf{x}\in\Omega_s\\ 0 & \text{at } \mathbf{x}\notin\Omega_s\end{cases}$$

the Eq. (5) is transformed into a simple local boundary integral equation

$$\int_{\partial\Omega_s^i}\overline{q}(\mathbf{x},s)d\Gamma-\int_{\Omega_s^i}\rho(\mathbf{x})c(\mathbf{x})s\overline{\theta}(\mathbf{x},s)d\Omega =-\int_{\Omega_s^i}\overline{F}(\mathbf{x},s)d\Omega. \quad (6)$$

Equation (6) is recognized as the flow balance condition of the subdomain. In the steady-state case there is no domain integration involved in the left hand side of this local boundary integral equation. If the assumption of zero body heat sources is made, the pure boundary integral formulation is obtained.

3 Meshless approximation and numerical solution

In general, a meshless method uses a local interpolation to represent the trial function with

the values (or the fictitious values) of the unknown variable at some randomly located nodes. The moving least-squares (MLS) approximation [Atluri (2004)] is used in the present analysis. To approximate the distribution of the Laplace transform of temperature over a number of randomly located nodes $\{\mathbf{x}^a\}$, $a = 1,2,...,n$, the MLS approximant $\overline{\theta}^h(\mathbf{x},s)$ of $\overline{\theta}$, is defined by

$$\overline{\theta}^h(\mathbf{x},s) = \mathbf{p}^T(\mathbf{x})\mathbf{a}(\mathbf{x},s), \tag{7}$$

where $\mathbf{p}^T(\mathbf{x}) = \left[p^1(\mathbf{x}), p^2(\mathbf{x}), ..., p^m(\mathbf{x})\right]$ is a complete monomial basis of order m; and $\mathbf{a}(\mathbf{x})$ is a vector containing the coefficients $a^j(\mathbf{x})$, $j = 1,2,...,m$which are functions of the space coordinates $\mathbf{x} = [x_1, x_2, x_3]^T$. In 3D problems, the linear basis is defined as

$$\mathbf{p}^T(\mathbf{x}) = [1, x_1, x_2, x_3], \tag{8}$$

and the quadratic basis is defined as

$$\mathbf{p}^T(\mathbf{x}) = \left[1, x_1, x_2, x_3, (x_1)^2, (x_2)^2, (x_3)^2, x_1x_2, x_1x_3, x_3x_2\right]. \tag{9}$$

The coefficient vector $\mathbf{a}(\mathbf{x})$ is determined by minimizing a weighted discrete L_2-norm defined as

$$J(\mathbf{x}) = \sum_{a=1}^{n} w^a(\mathbf{x}) \left[\mathbf{p}^T(\mathbf{x}^a)\mathbf{a}(\mathbf{x},s) - \hat{\theta}^a(s)\right]^2, \tag{10}$$

where $w^a(\mathbf{x})$ is the weight function associated with the node a with $w^a(\mathbf{x}) > 0$. Recall that n is the number of nodes in the support domain for which the weight function $w^a(\mathbf{x}) > 0$ and $\hat{\theta}^a(s)$ are the fictitious nodal values, but not the nodal values of the unknown trial function $\overline{\theta}^h(\mathbf{x},s)$ in general. The stationary condition of J in eq. (10) with respect to $\mathbf{a}(\mathbf{x},s)$,

$$\partial J/\partial \mathbf{a} = 0,$$

leads to the following linear relation between $\mathbf{a}(\mathbf{x},s)$ and $\hat{\theta}(s)$

$$\mathbf{A}(\mathbf{x})\mathbf{a}(\mathbf{x},s) - \mathbf{B}(\mathbf{x})\hat{\theta}(s) = 0, \tag{11}$$

where

$$\mathbf{A}(\mathbf{x}) = \sum_{a=1}^{n} w^a(\mathbf{x})\mathbf{p}(\mathbf{x}^a)\mathbf{p}^T(\mathbf{x}^a),$$

$$\mathbf{B}(\mathbf{x}) = \left[w^1(\mathbf{x})\mathbf{p}(\mathbf{x}^1), w^2(\mathbf{x})\mathbf{p}(\mathbf{x}^2), ..., w^n(\mathbf{x})\mathbf{p}(\mathbf{x}^n)\right]. \tag{12}$$

The MLS approximation is well defined only when the matrix $\mathbf{A}$ in eq. (11) is non-singular. A necessary condition to satisfy this requirement is that at least m weight functions are non-zero (i.e. $n \geq m$) for each sample point $\mathbf{x} \in \Omega$. The solution of eq. (11) for $\mathbf{a}(\mathbf{x},s)$ and a subsequent substitution into eq. (7) lead to the following relation

$$\overline{\theta}^h(\mathbf{x},s) = \mathbf{\Phi}^T(\mathbf{x}) \cdot \hat{\theta}(s) = \sum_{a=1}^{n} \phi^a(\mathbf{x})\hat{\theta}^a(s), \tag{13}$$

where

$$\mathbf{\Phi}^T(\mathbf{x}) = \mathbf{p}^T(\mathbf{x})\mathbf{A}^{-1}(\mathbf{x})\mathbf{B}(\mathbf{x}). \tag{14}$$

In eq. (14), $\phi^a(\mathbf{x})$ is usually referred to as the shape function of the MLS approximation corresponding to the nodal point $\mathbf{x}^a$. From eqs. (12) and (14), it can be seen that $\phi^a(\mathbf{x}) = 0$ when $w^a(\mathbf{x}) = 0$. In practical applications, $w^a(\mathbf{x})$ is often chosen such that it is non-zero over the support of the nodal point $\mathbf{x}_i$. The support of the nodal point $\mathbf{x}^a$ is usually taken to be a sphere of the radius r_i centred at $\mathbf{x}^a$ (see Fig. 1). The radius r_i is an important parameter of the MLS approximation because it determines the range of the interaction (coupling) between the degrees of freedom defined at considered nodes.

A 4^{th}-order spline-type weight function is applied in the present work

$$w^a(\mathbf{x}) = \begin{cases} 1 - 6\left(\frac{d^a}{r^a}\right)^2 + 8\left(\frac{d^a}{r^a}\right)^3 - 3\left(\frac{d^a}{r^a}\right)^4 & 0 \leq d^a \leq r^a \\ 0 & d^a \geq r^a \end{cases}, \tag{15}$$

where $d^a = \|\mathbf{x} - \mathbf{x}^a\|$ and r^a is the radius of the spherical support domain. With eq. (15), the C^1-continuity of the weight function is ensured over the entire domain, therefore the continuity condition of the heat flux is satisfied.

The partial derivatives of the MLS shape functions are obtained as [Atluri (2004)]

$$\phi^a_{,k} = \sum_{j=1}^{m} \left[p^j_{,k} (\mathbf{A}^{-1}\mathbf{B})^{ja} + p^j (\mathbf{A}^{-1}\mathbf{B}_{,k} + \mathbf{A}^{-1}_{,k}\mathbf{B})^{ja} \right], \tag{16}$$

wherein $\mathbf{A}^{-1}_{,k} = \left(\mathbf{A}^{-1}\right)_{,k}$ represents the derivative of the inverse of $\mathbf{A}$ with respect to x_k, which is given by

$$\mathbf{A}^{-1}_{,k} = -\mathbf{A}^{-1}\mathbf{A}_{,k}\mathbf{A}^{-1}.$$

The directional derivatives of $\overline{\theta}(\mathbf{x},s)$ are approximated in terms of the same nodal values as

$$\frac{\partial \overline{\theta}^h}{\partial n}(\mathbf{x},s) = n_k(\mathbf{x}) \sum_{a=1}^{n} \hat{\theta}^a(s) \phi^a_{,k}(\mathbf{x}). \tag{17}$$

Then, the Laplace transform of the heat flux is approximated by

$$\overline{q}(\mathbf{x},s) = k_{ij}(\mathbf{x}) n_i(\mathbf{x}) \sum_{a=1}^{n} \hat{\theta}^a(s) \phi^a_{,j}(\mathbf{x}). \tag{18}$$

The local integral equation, eq. (6), for 3D problems if the source point $\mathbf{x}^i$ is located inside Ω yields the following set of equations:

$$\sum_{a=1}^{n} \left(\int_{\partial\Omega^i_s} \mathbf{n}^T \mathbf{K}(\mathbf{x}) \mathbf{P}^a(\mathbf{x}) d\Gamma - \int_{\Omega^i_s} \rho c s \phi^a(\mathbf{x}) d\Omega \right) \hat{\theta}^a(s) = -\int_{\Omega^i_s} \overline{F}(\mathbf{x},s) d\Omega \tag{19}$$

where

$$\mathbf{K}(\mathbf{x}) = \begin{bmatrix} k_{11} & k_{12} & k_{13} \\ k_{12} & k_{22} & k_{23} \\ k_{13} & k_{23} & k_{33} \end{bmatrix}, \quad \mathbf{P}^a(\mathbf{x}) = \begin{bmatrix} \phi^a_{,1} \\ \phi^a_{,2} \\ \phi^a_{,3} \end{bmatrix},$$

$$\mathbf{n}^T = (n_1, n_2, n_3).$$

It should be noted that there are neither Lagrange multipliers nor penalty parameters introduced into the local weak form in eq. (4) because the essential boundary conditions on $\Gamma^i_{s\theta}$ can be imposed directly using the interpolation approximation eq. (13):

$$\sum_{a=1}^{n} \phi^a(\mathbf{x}) \hat{\theta}^a(s) = \tilde{\overline{\theta}}(\mathbf{x}^i, s) \text{ for } \mathbf{x}^i \in \Gamma^i_{s\theta} \tag{20}$$

where $\tilde{\overline{\theta}}(\mathbf{x}^i, s)$ is the Laplace transform of temperature prescribed on the boundary $\Gamma^i_{s\theta}$ for boundary conditions given in eq. (2).

Natural boundary conditions for the heat flux are satisfied on Γ^i_{sq} by collocation of the approximate expression eq. (18) at $\mathbf{x}^i$

$$\sum_{a=1}^{n} k_{lj}(\mathbf{x}^i) n_l \phi^a_{,j}(\mathbf{x}^i) \hat{\theta}^a(s) = \tilde{\overline{q}}(\mathbf{x}^i, s) \text{ for } \mathbf{x}^i \in \Gamma^i_{sq}. \tag{21}$$

If convective boundary conditions are considered and the temperature of the fluid medium outside has Heaviside time variation, $\theta_e(\mathbf{x},t) = \theta_{e0}(\mathbf{x}) H(t-0)$, the collocation equation has a form

$$\sum_{a=1}^{n} k_{lj}(\mathbf{x}^i) n_l \phi^a_{,j}(\mathbf{x}^i) \hat{\theta}^a(s) + \sum_{a=1}^{n} h(x) \phi^a(\mathbf{x}^i) \hat{\theta}^a(s) = h(\mathbf{x}^i) \theta_{e0}(\mathbf{x}^i)/s \text{ for } \mathbf{x}^i \in \Gamma^i_3 \tag{22}$$

The final system of algebraic equations for unknown Laplace transform temperature is created from eq. (19) at interior nodes and the corresponding collocation equation at boundary nodes. The time-dependent values of the transformed quantities in the previous consideration can be obtained by an inverse transform. There are many inversion methods available for the inverse Laplace transform. In the present analysis, the sophisticated Stehfest's algorithm [Stehfest (1970)] for the numerical inversion is used. If $\overline{f}(s)$ is the Laplace transform of $f(t)$, an approximate value f_a of $f(t)$ for a specific time t is given by

$$f_a(t) = \frac{\ln 2}{t} \sum_{i=1}^{N} v_i \overline{f}\left(\frac{\ln 2}{t} i\right), \tag{23}$$

where

$$v_i = (-1)^{N/2+i} \sum_{k=[(i+1)/2]}^{\min(i,N/2)} \frac{k^{N/2}(2k)!}{(N/2-k)!k!(k-1)!(i-k)!(2k-i)!}. \tag{24}$$

In the numerical analysis here, N = 10 is used for double precision arithmetic. This means that for each time t, it is needed to solve N boundary value problems for the corresponding Laplace parameters$s = i\ln 2/t$, with $i = 1,2,...,N$. If M denotes the number of the time instants in which we are interested to know $f(t)$, the number of the Laplace transform solutions $\overline{f}(s_j)$ is then $M \times N$.

4 Numerical examples

In this section, numerical results will be presented to illustrate the implementation and effectiveness of the MLPG method for transient heat conduction problems. First, homogeneous material properties and steady-state boundary conditions are considered. An anisotropic cube as shown in Fig. 2 is analyzed; for the purpose of illustration, a relatively coarse node distribution is shown here , with typical mixed boundary conditions on the surfaces.

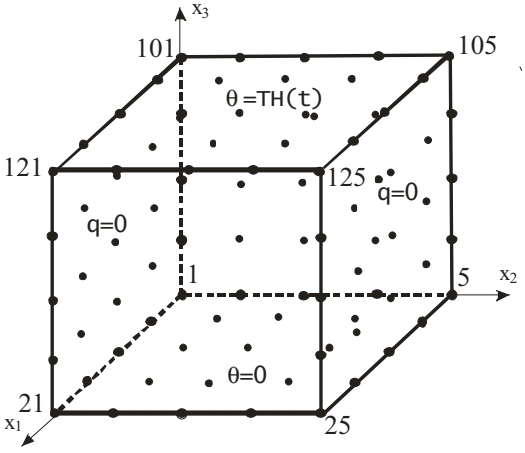

Figure 2: Mixed boundary conditions for analyzed cube

In the first example, Example (1), steady-state, Dirichlet boundary conditions are prescribed over the entire surface of the cube. The numerical values chosen are for a cube with side $a = 10m$ and thermal conductivity tensor components: $k_{11} = k_{22} = k_{33} = 1 \times 10^{-4}$ and $k_{23} = 0.2 \times 10^{-4} m^2 s^{-1}$; the other terms in the thermal conductivity matrix being zero. In the MLS approximation, a regular node distribution with a total 1331 nodes is used here. The radius of the spherical subdomain is considered as $r_{loc} = 0.8m$. This simple example was considered as a verification of the accuracy of the present method. It can be easily shown that the analytical solution

$$\theta = x_2^2 + x_2 - 5x_2x_3 + x_1x_3$$

satisfies the governing equation (1) under steady-state conditions for the thermal conductivity values considered. Essential boundary conditions are prescribed on the surfaces, with the temperatures as obtained from the analytical solution above. The numerical results can be compared with analytical ones. The Sobolev norm of the errors for the temperatures obtained

$$r_\theta = \frac{\|\theta^{num} - \theta^{exact}\|}{\|\theta^{exact}\|} \times 100\% \text{ with } \|\theta\| = \left(\int_\Omega \theta\theta^d \Omega \right)^{1/2}$$

is 0.37%. The temperature distributions at the mid-plane of the cube $x_3/a = 0.5$ and at two different coordinates $x_1/a = 0.5$ and 0.9 along the x_2-coordinate direction are shown in Fig. 3. It can be seen that there is excellent agreement between the MLPG and analytical results.

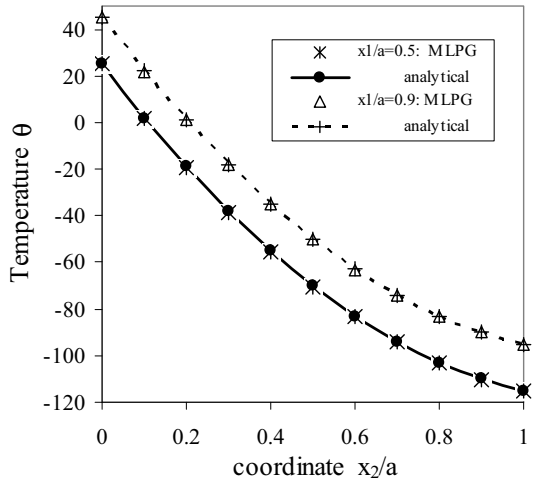

Figure 3: Temperature distribution in a homogeneous anisotropic cube –Ex. (1)

In the second numerical example, Example (2), mixed steady-state boundary conditions are considered. A homogeneous anisotropic cube domain $(10 \times 10 \times 10)$ with vanishing heat flux on lateral walls, and prescribed temperature $\theta = 0$ and $\theta = 1$ on the bottom and top surfaces, respectively, is considered (Fig. 2). The values of the thermal conductivity tensor components are: $k_{11} = k_{33} = 1$, $k_{22} = 1.5$, $k_{23} = k_{32} = 0.5$, $k_{13} = k_{12} = 0$. In the stated 3D boundary value problem, the temperature distribution is not dependent on x_1-coordinate. Therefore, it can be analyzed as a 2D problem as has been carried out by Sladek et al. (2004a) on the same problem; the results can thus be compared. The temperature variations along the x_3 coordinate direction on the left $(x_2/a = 0)$ and right $(x_2/a = 1)$ lateral sides are given in Fig. 4, where again, very good agreement between the 2D and 3D results is observed. It should be noted that in an isotropic cube under the same boundary conditions, a linear variation of the temperature with x_3 coordinate will be obtained. Nonlinear variation of temperature in Fig. 4 is due to the anisotropic properties of the heat conduction parameters.

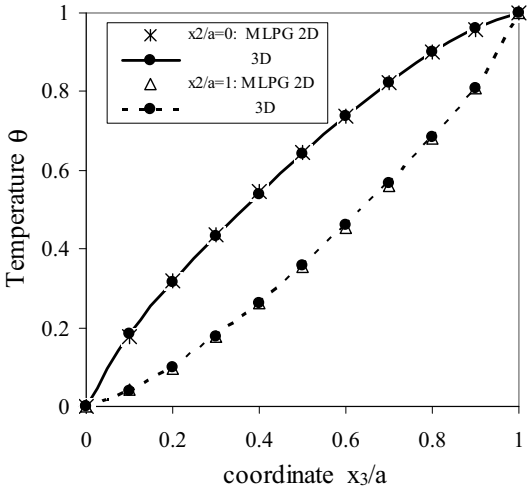

Figure 4: Temperature variations with x_3 coordinate in a homogeneous anisotropic cube – Ex. (2)

In Example (3), the same geometry and boundary conditions as in Example (2) are considered for a non-homogeneous (FGM) cube, where $k_{33}(x_3) = 1 + x_3/a$, $k_{22} = 1.5$, $k_{11} = 1.$,$k_{23} = 0.5$, $k_{13} = k_{12} = 0$. Again, the temperature distribution is not dependent on the x_1 coordinate and the 2D problem has been tested in the authors' previous work [Sladek et al. (2004a)]. The results for the temperature variations along the x_3 coordinate direction on the left $(x_2/a = 0.)$ and right $(x_2/a = 1.)$ lateral sides are given in Fig. 5, where the very good agreement of the results obtained from 2D and 3D analyses is observed once again. Also shown in this figure are the corresponding results, in dashed lines, for the homogeneous case. If the thermal conductivity k_{33} is increasing linearly with x_3 coordinate, a higher temperature distribution is to be expected for the FGM than for a homogeneous material. This is reflected by the curves corresponding to the former case being shifted to the left with respect to those for the latter case.

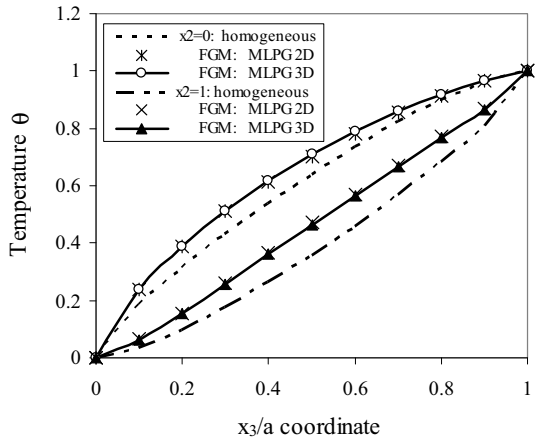

Figure 5: Temperature variations with x_3/a in an anisotropic FGM cube – Ex. (3)

After having tested the present MLPG method above, it will now be applied to problems of an anisotropic body with more general variations of the material properties with respect to the Cartesian coordinates, which cannot be solved as 2D problems as was possible in the previous two numerical examples. Consider, in Example (4), a homogeneous anisotropic cube domain $(10 \times 10 \times 10)$ with vanishing heat flux on its lateral walls, and prescribed temperature $\theta = 0$ and $\theta =$ 1on the bottom and top surfaces, respectively;

the domain has the following heat conductivities: $k_{11} = k_{33} = 1, k_{22} = 1.5, k_{12} = k_{13} = k_{23} = 0.5$. In this case, it is clear that the temperature distribution will not be independent of the x_1-coordinate. Figure 6 shows the computed temperature variation along the x_3 coordinate at left and right lateral sides of two planes $x_1/a = 0.$ and 1, respectively. The qualitative features of the trends are similar to those seen in the previous case where some symmetry of material properties has been considered.

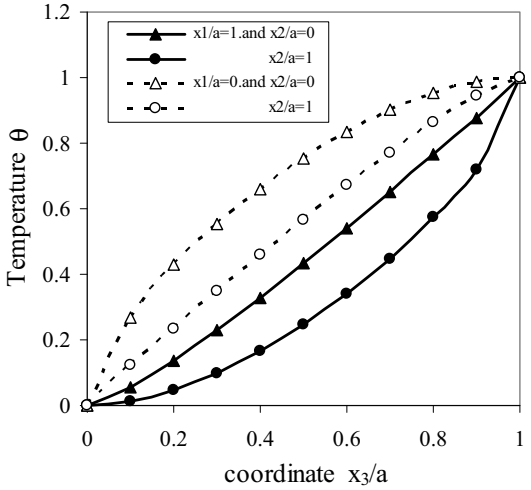

Figure 6: Temperature variations with x_3/a in a homogeneous anisotropic cube – Ex.(4)

A functionally graded material is treated next, in Example (5). The same cube geometry and boundary conditions as in Example 4 is considered, but with thermal conductivities of the domain having the following values:$k_{11} = 1., k_{22} = 1.5$, $k_{33}(x_3) = 1 + x_3/a$, $k_{12} = k_{13} = k_{23} = 0.5$. Figures 7 and 8 show the computed variations of the temperature in the cube with the x_3 coordinate direction at = 0 and x_2/a= 1 on the two lateral sides, x_1= 1 and x_1= 0, respectively. Also shown for comparison are the corresponding results for the homogeneous case seen in the previous example; the effects of non-homogeneity of the material property are clearly evident.

Numerical examples of the application of the present method to transient heat conduction are presented next. Homogeneous isotropic material property is considered first, in Example (6), with

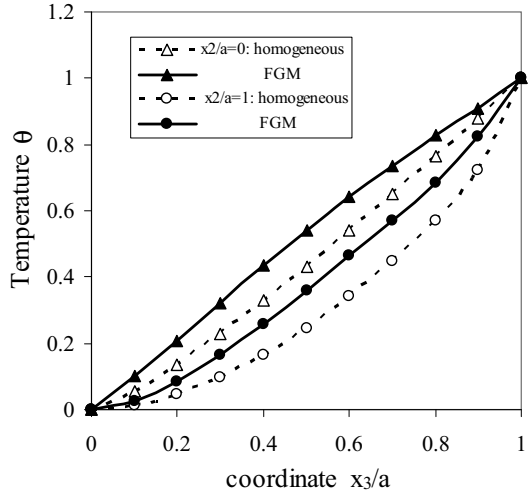

Figure 7: Temperature variations with x_3/a in plane $x_1/a = 1.$ of an anisotropic FGM cube – Ex. (5)

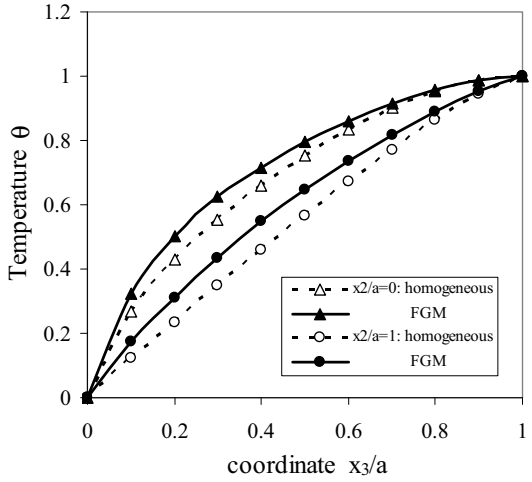

Figure 8: Temperature variations with x_3/a in plane $x_1/a = 0.$ of an anisotropic FGM cube – Ex. (5)

$k_{11} = k_{22} = k_{33} = 1, k_{12} = k_{13} = k_{23} = 0$. The same boundary conditions as in the previous case are considered but with a thermal shock $\theta_0 H(t-0)$ represented by the Heaviside time step function applied on the top surface of the cube (Fig. 2). The temperature distribution has to be independent on x_1 and x_2 coordinates. Due to this independence, the problem can also be analyzed in 2D, so that the numerical results can be compared.

The MLPG method is used to solve the boundary value problems in the Laplace transform domain. The Stehfest inversion method is applied to obtain the time-dependent solutions at three various planes $x_3/a = 0.1$, 05, 0.8. The time variations of the temperature are shown in Fig. 9 where one can observe the very good agreement of the results obtained from 2D and 3D analyses.

In Example (7), an anisotropic analysis of the cube with the same set of heat conductivities for the domain used earlier: $k_{11} = k_{33} = 1$, $k_{22} = 1.5$, $k_{12} = k_{13} = k_{23} = 0.5$, is carried out. Time variations of temperature at $x_3/a = 0.8$ and $x_2/a = 0.5$ on the front and back surfaces of the cube are presented in Fig. 10. Note that at large time instants, the temperatures approach the steady-state values, as to be expected.

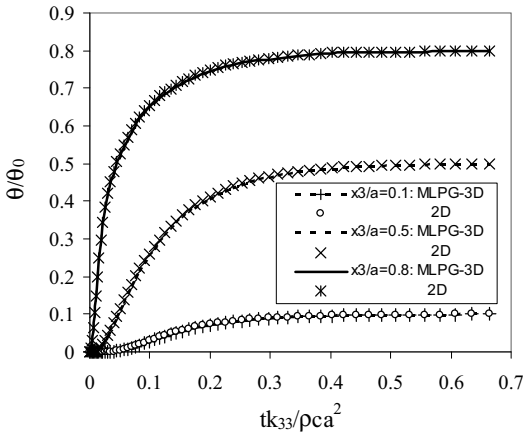

Figure 9: Time variations of the temperature in an isotropic cube – Ex. (6)

In the next example, Example (8), the cube in Example (7) is treated as being an anisotropic FGM with the following set of thermal conductivities: $k_{33}(x_3) = 1 + x_3/a$, $k_{22} = 1.5$, $k_{11} = 1.$, $k_{23} = 0.5$, $k_{13} = k_{12} = 0.$. Figure 11 shows a comparison of the time variations of temperatures in the homogeneous anisotropic and FGM cubes; the temperature values are computed at $x_3/a = 0.2$, the values of the two x_1 coordinate positions are given in the figure. The temperature on the front surface, $x_1/a = 1$, is higher than that on the back surface, $x_1/a = 0$. At large time instants, the temperature approach the steady-state values given in Fig. 7 and 8. Very good agreement between the computed quantities is observed.

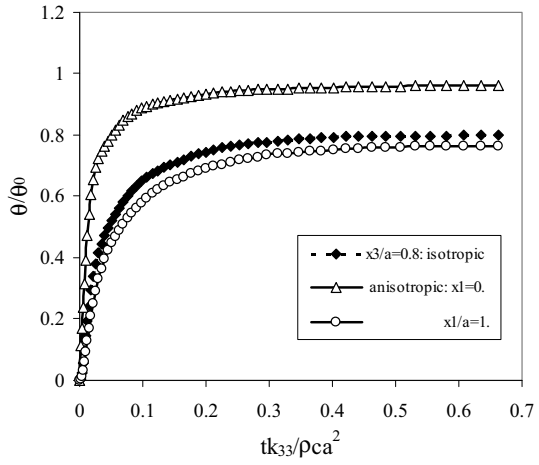

Figure 10: Time variations of the temperature in a homogeneous anisotropic cube – Ex. (7)

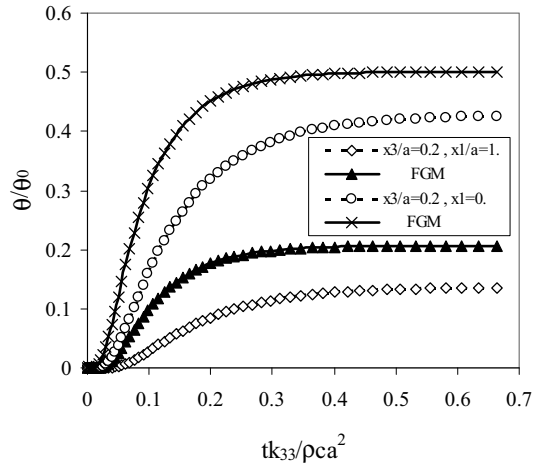

Figure 11: Time variations of the temperature in an anisotropic cube – Ex. (8)

Finally, in Example (9), a convection boundary condition on the cube is considered. On the bottom and lateral surfaces of the cube there is vanishing heat flux, and on the top surface, heat convection with the heat transfer coefficient $h = 1.0W/m^2K$, occurs. The temperature of the fluid medium outside has Heaviside time variation, $\theta_e(\mathbf{x},t) = \theta_0(\mathbf{x})H(t-0)$. Isotropic material property is considered here, with $k_{11} = k_{22} =$

$k_{33} = 1$, $k_{13} = k_{12} = k_{23} = 0.$, since analytical solution in a layer is available for comparison. The cube with vanishing heat fluxes on lateral surfaces can be considered as a layer with the thickness $L = a = 10m$; the analytical solution for this problem is [Carslaw and Jaeger (1959)]

$$\theta(x_3,t) = \theta_0 \left\{ 1 - 2m \sum_{i=1}^{\infty} \frac{\sin\beta_i \cos\left(\frac{\beta_i x_3}{L}\right) \exp\left(\frac{-\beta_i^2 \alpha t}{L^2}\right)}{\beta_i \left[m + \sin^2\beta_i\right]} \right\}, \tag{25}$$

where $\alpha = k_{33}/\rho c = 1$ and the eigenvalues β_i are the roots of the transcendental equations $\frac{\beta \sin\beta}{\cos\beta} - m = 0$ with $m = \frac{hL}{k_{33}}$.

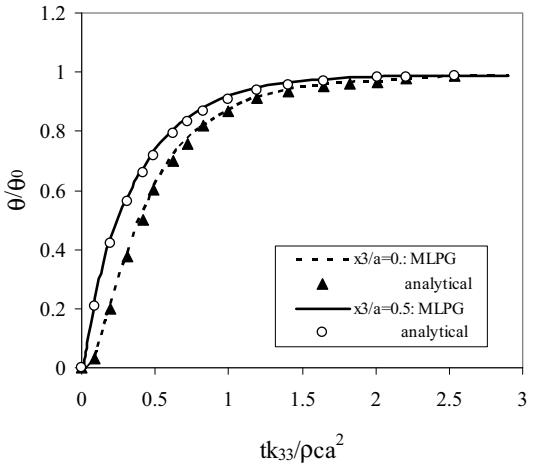

Figure 12: Time variations of the temperature in an isotropic cube with heat convection – Ex. (9)

Figure 12 shows the time variation of the temperature in the analyzed cube at x_3/a = 0 and x_3/a = 1. The numerical results are compared with the analytical ones and it can be seen that there is very good agreement indeed.

5 Conclusions

A local boundary integral equation formulation in Laplace transform-domain with meshless approximation has been successfully implemented to solve 3D initial-boundary value problems for transient heat conduction in anisotropic, continuously non-homogeneous solids.

The Heaviside step function is used as test functions in the local symmetric weak form, leading to the derivation of the local boundary-domain integral equations. In contrast to conventional boundary integral equation methods, all the integrands in the present formulation are regular. Thus, no special integration techniques are required to evaluate the integrals.

The analyzed domain is divided into small overlapping spherical subdomains on which the local boundary integral equations are applied. The proposed methods are truly meshless methods, wherein no elements or background cells are involved in either the interpolation or the integration. The Moving Least-Squares (MLS) scheme is adopted for approximating the physical quantities.

The main advantage of the present method is its simplicity and generality in comparison to, say, the conventional BEM. The method is particularly promising for problems which cannot be solved by the conventional BEM when the fundamental solutions are not available. However, in its current development, the computational time in the proposed method is larger since there are many more nodes involved and the shape functions in the MLS approximation are significantly more complex than in BEM or FEM using simple polynomials. By employing a mixed formulation [Atluri et al. (2004), (2006b)], the radius of the support domain can be reduced to obtain the same accuracy as in the traditional approximation. A smaller size of the support domain decreases the bandwidth of the final system matrix and the computational effort is thus significantly reduced. It is proposed as a future work, that a mixed formulation be applied to the present 3D heat conduction analysis.

The proposed method can be further extended to nonlinear problems, where meshless approximations may have certain advantages over the conventional domain-type discretization approaches.

Acknowledgement: The authors acknowledge the support by the Slovak Science and Technology Assistance Agency registered under num-

ber APVV-51-021205, APVV-0427-07, the Slovak Grant Agency VEGA-2/6109/27, VEGA-1/4128/07.

References

Atluri, S.N. (2004): *The Meshless Method(MLPG) for Domain & BIE Discretizations*, 688 pages, Tech Science Press, Forsyth, GA.

Atluri, S.N.; Zhu, T. (1998): A New Meshless Local Petrov-Galerkin (MLPG) Approach in Computational Mechanics, *Computational Mechanics*, 22: 117-127,

Atluri S.N., ; Shen S. (2002a): The Meshless Local Petrov-Galerkin (MLPG) Method: A Simple & Less-costly Alternative to the Finite Element and Boundary Element Methods, *CMES: Computer Modeling in Engineering & Sciences*, 3: 11-52.

Atluri, S.N.; Shen, S. (2002b): *The Meshless Local Petrov-Galerkin (MLPG) Method*, Tech Science Press, Forsyth, GA.

Atluri, S.N.; Sladek, J.; Sladek, V.; Zhu, T. (2000): The local boundary integral equation (LBIE) and its meshless implementation for linear elasticity. *Comput. Mech*., 25: 180-198.

Atluri, S.N.; Han, Z.D.; Shen, S. (2003): Meshless local Petrov-Galerkin (MLPG) approaches for solving the weakly-singular traction & displacement boundary integral equations. *CMES: Computer Modeling in Engineering & Sciences*, 4: 507-516.

Atluri S.N., Han Z.D., Rajendran A.M. (2004): A new implementation of the meshless finite volume method, through the MLPG "Mixed" approach , *CMES: Computer Modeling in Engineering & Sciences*: 6: 491-513.

Atluri, S.N.; Liu, H.T.; Han, Z.D. (2006a): Meshless local Petrov-Galerkin (MLPG) mixed collocation method for elasticity problems. *CMES: Computer Modeling in Engineering & Sciences*, 14 (3): 141-152.

Atluri, S.N.; Liu, H.T.; Han, Z.D. (2006b): Meshless local Petrov-Galerkin (MLPG) mixed finite difference method for solid mechanics. *CMES: Computer Modeling in Engineering & Sciences*, 15 (1): 1-16.

Belytschko, T.; Krogauz, Y.; Organ, D.; Fleming, M.; Krysl, P. (1996): Meshless methods; an overview and recent developments. *Comp. Meth. Appl. Mech. Engn.*, 139: 3-47.

Brebbia, C.A.; Telles, J.C.F.; Wrobel, L.C. (1984): *Boundary Element Techniques*, Springer.

Carslaw, H.S.; Jaeger, J.C. (1959): *Conduction of Heat in Solids*, Clarendon, Oxford.

Chang, Y.P.; Kang, C.S.; Chen, D.J. (1973): The use of fundamental Green's functions for the solution of problems of heat conduction in anisotropic media. *J. Heat and Mass Transfer*, 16: 1905-1918.

Ching, H.K.; Chen, J.K. (2006): Thermomechanical analysis of functionally graded composites under laser heating by the MLPG method. *CMES: Computer Modeling in Engineering & Sciences*, 13 (3): 199-217.

Erdogan, F.; Wu, B.H. (1996): Crack problems in FGM layers under thermal stresses. *J. Thermal Stresses*, 19: 237-265.

Gao, L.; Liu, K.; Liu, Y. (2006): applications of MLPG method in dynamic fracture problems. *CMES: Computer Modeling in Engineering & Sciences*, 12 (3): 181-195.

Han, Z.D.; Atluri, S.N. (2004a): Meshless local Petrov-Galerkin (MLPG) approaches for solving 3D problems in elasto-statics. *CMES: Computer Modeling in Engineering & Sciences*, 6: 169-188.

Han, Z.D.; Atluri, S.N. (2004b): A meshless local Petrov-Galerkin (MLPG) approach for 3-dimensional elasto-dynamics. *CMC: Computers, Materials & Continua*, 1: 129-140.

Han, Z.D.; Rajendran, A.N.; Atluri, S.N. (2005): Meshless Local Petrov-Galerkin (MLPG) approaches for solving nonlinear problems with large deformations and rotations. *CMES: Computer Modeling in Engineering & Sciences*, 10 (1): 1-12.

Jin, Z.H. (2002): An asymptotic solution of temperature field in a strip of a functionally graded material. *Int. Comm. Heat Mass Transfer*, 29: 887-895.

Jin, Z.H.; Noda, N. (1993): An internal crack parallel to the boundary of a nonhomogeneous half plane under thermal loading. *Int. J. Eng. Sci.*, 31: 793-806.

Jin, Z.H.; Batra, R.C. (1996): Stress intensity relaxation at the tip of an edge crack in a functionally graded material subjected to a thermal shock. *J. Thermal Stresses*, 19: 317-339.

Jin, Z.H.; Paulino, G.H. (2001): Transient thermal stress analysis of an edge crack in a functionally graded material. *Int. J. Fract.*, 107: 73-98.

Kim, J.H.; Paulino, G.H. (2002): Isoparametric graded finite elements for nonhomogeneous isotropic and orthotropic materials. *J. Appl. Mech.*, 69: 502-514.

Long, S.Y.; Atluri, S.N. (2002): A meshless local Petrov Galerkin method for solving the bending problem of a thin plate. *CMES: Computer Modeling in Engineering & Sciences*, 3: 11-51.

Mikhailov, S.E. (2002): Localized boundary-domain integral formulations for problems with variable coefficients. *Engn. Analysis with Boundary Elements*, 26: 681-690.

Miyamoto, Y.; Kaysser, W.A.; Rabin, B.H.; Kawasaki, A.; Ford, R.G. (1999): *Functionally Graded Materials; Design, Processing and Applications*, Kluwer Academic Publishers, Dordrecht.

Noda, N.; Jin, Z.H. (1993): Thermal stress intensity factors for a crack in a strip of a functionally gradient material. *Int. J. Solids and Struct.* , 30: 1039-1056.

Noda, N.; Jin, Z.H. (1994): A crack in functionally gradient materials under thermal shock. *Arch. Appl. Mech.*, 64: 99-110.

Sladek, J.; Sladek, V.; Atluri, S.N. (2000): Local boundary integral equation (LBIE) method for solving problems of elasticity with nonhomogeneous material properties, *Computational Mechanics*, 24: 456-462.

Sladek, J.; Sladek, V.; Atluri, S.N. (2001): A pure contour formulation for the meshless local boundary integral equation method in thermoelasticity. *CMES: Computer Modeling in Engineering & Sciences*, 2: 423-434.

Sladek, J.; Sladek, V.; Mang, H.A. (2002):Meshless formulations for simply supported and clamped plate problems. *Int. J. Num. Meth. Engn.*, 55: 359-375.

Sladek, J.; Sladek, V.; Van Keer, R. (2003a): Meshless local boundary integral equation method for 2D elastodynamic problems. *Int. J. Num. Meth. Engn.*, 57: 235-249.

Sladek, J.; Sladek, V.; Zhang, Ch. (2003b): Application of meshless local Petrov-Galerkin (MLPG) method to elastodynamic problems in continuously nonhomogeneous solids, *CMES: Computer Modeling in Engn. & Sciences*, 4: 637-648.

Sladek, J.; Sladek, V.; Zhang, Ch. (2003c): Transient heat conduction analysis in functionally graded materials by the meshless local boundary integral equation method. *Comput. Material Science*, 28: 494-504.

Sladek, J.; Sladek, V.; Krivacek, J.; Zhang, Ch. (2003d): Local BIEM for transient heat conduction analysis in 3-D axisymmetric functionally graded solids. *Comput. Mech.*, 32: 169-176.

Sladek, J.; Sladek, V.; Atluri, SN (2004a): Meshless local Petrov-Galerkin method for heat conduction problem in an anisotropic medium, *CMES: Computer Modeling in Engn. & Sciences*, 6: 309-318.

Sladek, J.; Sladek, V.; Zhang, Ch. (2004b): A meshless local boundary integral equation method for heat conduction analysis in nonhomogeneous solids, *Jour. Chinese Institute Engng.*, 27: 517-539.

Sladek, J.; Sladek, V.; Atluri, S.N. (2004c): Meshless local Petrov-Galerkin method in anisotropic elasticity. *CMES: Computer Modeling in Engn. & Sciences*, 6: 477-489.

Sladek, J.; Sladek, V.; Hellmich, Ch.; Eberhardsteiner, J. (2007a): Heat conduction analysis of 3D axisymmetric and anisotropic FGM bodies by meshless local Petrov-Galerkin method, *Computational Mechanics*, 39: 323-333.

Sladek, J.; Sladek, V.; Zhang, Ch.; Solek, P.; Pan, E. (2007b): Evaluation of fracture parameters in continuously nonhomogeneous piezoelectric solids. *International Journal of Fracture*, 145: 313-326.

Sladek, J.; Sladek, V.; Krivacek, J.; Aliabadi, M.H. (2007c): Local boundary integral equations for orthotropic shallow shells, *Int. J. Solids and Structures*, 44: 2285-2303.

Sladek, J.; Sladek, V.; Solek, P.; Wen, P.H. (2008): Thermal bending of Reissner-Mindlin plates by the MLPG. *CMES: Computer Modeling in Engineering & Sciences*, 28: 57-76.

Sellountos, E.J.; Vavourakis, V.; Polyzos, D. (2005): A new singular/hypersingular MLPG (LBIE) method for 2D elastostatics, *CMES: Computer Modeling in Engineering & Sciences*, 7: 35-48.

Soric, J.; Li, Q.; Atluri, S.N. (2004): Meshless local Petrov-Galerkin (MLPG) formulation for analysis of thick plates. *CMES: Computer Modeling in Engineering & Sciences*, 6: 349-357.

Stehfest, H. (1970): Algorithm 368: numerical inversion of Laplace transform. *Comm. Assoc. Comput. Mach.*, 13: 47-49.

Suresh, S.; Mortensen A. (1998): *Fundamentals of Functionally Graded Materials.* Institute of Materials, London.

Sutradhar, A.; Paulino, G.H.; Gray, L.J. (2002): Transient heat conduction in homogeneous and non-homogeneous materials by the Laplace transform Galerkin boundary element method. *Engn. Analysis with Boundary Elements*, 26: 119-132.

Tanaka, M.; Tanaka, K. (1980): Transient heat conduction problems in inhomogeneous media discretized by means of boundary-volume element. *Nucl. Eng. Des.*, 60: 381-387.

Yuan, W.; Chen, P.; Liu, K. (2007): A new quasi-unsymmetric sparse linear systems solver for Meshless Local Petrov-Galerkin method (MLPG). *CMES: Computer Modeling in Engineering & Sciences*, 17 (2): 115-134.

Wu, X.H.; Shen, S.P.; Tao, W.Q. (2007): Meshless Local Petrov-Galerkin collocation method for two-dimensional heat conduction problems. *CMES: Computer Modeling in Engineering & Sciences*, 22 (1): 65-76.

Zhu, T.; Zhang, J.D.; Atluri, S.N. (1998): A local boundary integral equation (LBIE) method in computational mechanics, and a meshless discretization approach. *Comput. Mech.*, 21: 223-235.